

Integral transform solutions for atmospheric pollutant dispersion

Gevaldo L. de Almeida · Luiz C. G. Pimentel · Renato M. Cotta

Received: 5 April 2006 / Accepted: 23 August 2006 / Published online: 27 January 2007
© Springer Science + Business Media B.V. 2007

Abstract A transient two-dimensional advection–diffusion model describing the turbulent dispersion of pollutants in the atmosphere has been solved via the Generalized Integral Transform Technique (GITT), by two different schemes. The first approach performs numerical integration of the transformed system using available routines for initial value problems with automatic error control. In spite of the time-consuming character of such a scheme, its flexibility allows the handling of problems involving time-dependent meteorological parameters such as wind speed and eddy diffusivities. The second approach works fully analytically being thus intrinsically more robust and economic, although not directly applicable in dealing with time-dependent parameters. For the test problem used in this work, both methods agree very well with each other, as well as with a known analytical solution for a simpler formulation used as benchmark. The impact of the longitudinal diffusivity on the stiffness of the ordinary differential equation (ODE) system arising from the integral transformation has been assessed through the processing time demanded to solve it when the numerical approach is used. The observed CPU

times show that the analytical approach is clearly preferable unless the problem involves time-dependent parameters.

Keywords integral transforms · dispersion · hybrid methods · advection-diffusion · atmospheric pollution

1 Introduction

The Generalized Integral Transform Technique (GITT) is a well-known hybrid numerical–analytical approach that can efficiently handle diffusion and convection–diffusion partial differential formulations. It is based on expansions of the original potentials in terms of eigenfunctions and the solution is obtained through integral transformation in all but one of the independent variables, thus reducing the partial differential formulations to an ordinary differential system for the expansion coefficients, which can be then solved using numerical techniques or in some special cases, analytical procedures [1, 4, 7].

The GITT has been progressively developed and improved [4–6,] in the past two decades and mainly applied to heat and fluid flow problems, including nonlinear diffusion, boundary layer and Navier–Stokes formulations of convection–diffusion. The first application of the GITT addressing pollutant transport in the atmosphere recently carried out [10], by applying a single integral transformation to a two-dimensional transient advection–diffusion problem. The resulting one-dimensional system of coupled partial differential equations was then numerically solved. Later on, a similar problem was solved [2] by applying a double integral transformation to the differential formulation, previously filtered by a steady-state diffusive filter, changing it to a system of time-dependent ODEs which has been numerically solved as

G. L. de Almeida
Instituto de Engenharia Nuclear, IEN,
Comissão Nacional de Energia Nuclear, CNEN,
Rio de Janeiro, RJ, Brazil

L. C. G. Pimentel · R. M. Cotta
LAMMA/Departamento de Meteorologia,
Universidade Federal do Rio de Janeiro,
Rio de Janeiro, Brazil

R. M. Cotta (✉)
Center for Analysis and Simulations in Environmental
Engineering (CASEE), Universidade Federal do Rio de Janeiro,
LTTTC – PEM/COPPE/UFRJ,
Caixa Postal 68503 Cidade Universitaria,
Rio de Janeiro, RJ CEP 21945-970, Brazil
e-mail: cotta@serv.com.ufrj.br

well. Quite recently, Moreira et al. [12] and Wortman et al. [13] applied the GITT to a two-dimensional steady-state advection–diffusion problem of dispersion of pollutants in the atmosphere, solving the resulting system of ODEs by Laplace transforms rather than employing numerical techniques.

The present work addresses the solution via GITT of a transient two-dimensional advection–diffusion formulation describing the dispersion of pollutants in the atmosphere. The boundary condition at $x=0$, where a continuous source is located, is homogenized through a proper advective–diffusive filter.

After the double integral transformation, the resulting time-dependent ordinary differential equation (ODE) system was solved by two different approaches: (a) numerically, using the routine DIVPAG from the IMSL library; and (b) analytically, by performing the appropriate eigen-system analysis. The first approach is more general, because it can deal with problems involving time-dependent parameters such as wind speed and eddy diffusivities, while the second one is computationally more efficient but cannot directly handle such more involved problems.

The results emerging from both approaches agree very well not only with each other, but also with a known analytical solution of the proposed test problem. The required CPU times and the impact of the system stiffness on the computational cost were also assessed.

2 Problem formulation

The chosen test problem refers to a transient two-dimensional turbulent advection–diffusion model of an effluent in the atmosphere which is emitted by an elevated source such as a stack. The ground is assumed to be an impermeable barrier while the surface boundary layer is a fully permeable one.

An inert effluent starts suddenly to be continuously and regularly released at the height Z_e in an atmosphere where the time-dependent parameters, wind speed, vertical and longitudinal eddy diffusivities change with the height above ground level. The pollutant concentration is given by the solution of the partial differential system (1)–(6):

$$\frac{\partial C(X, Z, \tau)}{\partial \tau} + U(Z, \tau) \frac{\partial C(X, Z, \tau)}{\partial X} = \frac{\partial}{\partial Z} \left[K_{zz}(Z, \tau) \frac{\partial C(X, Z, \tau)}{\partial Z} \right] + K_{xx}(Z, \tau) \frac{\partial^2 C(X, Z, \tau)}{\partial X^2}, \quad 0 < Z < H, 0 < X < X_m, \tau > 0 \tag{1}$$

$$C(X, Z, \tau)|_{\tau=0} = 0 \tag{2}$$

$$\frac{\partial C(X, Z, \tau)}{\partial Z} \Big|_{Z=0} = 0 \tag{3}$$

$$C(X, Z, \tau)|_{Z=H} = 0 \tag{4}$$

$$C(X, Z, \tau)|_{X=0} = \frac{Q}{u(Z_e)} \delta(Z - Z_e) \tag{5}$$

$$\frac{\partial C(X, Z, \tau)}{\partial X} \Big|_{X=X_m} = 0 \tag{6}$$

where C is the effluent concentration, τ is the time elapsed, X is the downwind distance, $U(Z, \tau)$ is the wind speed, Z is the height above the ground, $K_{zz}(Z, \tau)$ is the vertical eddy diffusivity, $K_{xx}(Z, \tau)$ is the longitudinal eddy diffusivity, Z_e is the emission height, δ is Dirac delta function, H is the vertical domain, and X_m is the longitudinal domain.

The system (1)–(6) can be rewritten in dimensionless form as:

$$\frac{\partial c(x, z, t)}{\partial t} + A \cdot u(z, t) \frac{\partial c(x, z, t)}{\partial x} = \frac{\partial}{\partial z} \left[k_{zz}(z, t) \frac{\partial c(x, z, t)}{\partial z} \right] + B \cdot k_{xx}(z, t) \frac{\partial^2 c(x, z, t)}{\partial x^2}, \quad 0 < z < 1, \quad 0 < x < 1, \quad t > 0 \tag{7}$$

$$c(x, z, t)|_{t=0} = 0 \tag{8}$$

$$\frac{\partial c(x, z, t)}{\partial z} \Big|_{z=0} = 0 \tag{9}$$

$$c(x, z, t)|_{z=1} = 0 \tag{10}$$

$$c(x, z, t)|_{x=0} = \frac{1}{u(z_e)} \delta(z - z_e) \tag{11}$$

$$\frac{\partial c(x, z, t)}{\partial x} \Big|_{x=1} = 0 \tag{12}$$

using the groups

$$x = \frac{X}{X_m} \tag{13}$$

$$z = \frac{Z}{H} \tag{14}$$

$$t = \frac{K_{zz}(H)}{H^2} \tau \tag{15}$$

$$z_e = \frac{Z_e}{H} \tag{16}$$

$$c(x, z, t) = \frac{U(H) \cdot H}{Q} C(X, Z, \tau) \tag{17}$$

$$k_{zz}(z, t) = \frac{K_{zz}(Z, \tau)}{K_{zz}(H, \tau)} \tag{18}$$

$$k_{xx}(z, t) = \frac{K_{xx}(Z, \tau)}{K_{xx}(H, \tau)} \tag{19}$$

$$u(z, t) = \frac{U(Z, \tau)}{U(H, \tau)} \tag{20}$$

$$A = H^2 X_m^{-1} U(H, t) K_{zz}^{-1}(H, \tau) \tag{21}$$

$$B = H^2 X_m^{-2} K_{xx}(H, t) K_{zz}^{-1}(H, \tau) \tag{22}$$

System (7–12) is solved through the GITT after proper application of a steady-state filter $F(x, z)$ to homogenize the boundary condition at $x=0$, while maintaining the other boundary conditions homogeneous. This approach decomposes the potential into a transient filtered potential and a steady-state filter as follows:

$$c(x, z, t) = c^*(x, z, t) + F(x, z) \tag{23}$$

Replacing equation (23) into the system (7)–(12):

$$\begin{aligned} \frac{\partial c^*(x, z, t)}{\partial t} + A \cdot u(z, t) \frac{\partial c^*(x, z, t)}{\partial x} \\ = \frac{\partial}{\partial z} \left[k_{zz}(z, t) \frac{\partial c^*(x, z, t)}{\partial z} \right] \\ + B \cdot k_{xx}(z, t) \frac{\partial^2 c^*(x, z, t)}{\partial x^2} + G(x, z, t) \end{aligned} \tag{24}$$

$$\begin{aligned} G(x, z, t) = \frac{\partial}{\partial z} \left[k_{zz}(z, t) \frac{\partial F(x, z)}{\partial z} \right] \\ + B k_{xx}(z, t) \frac{\partial^2 F(x, z)}{\partial x^2} \\ - A \cdot u(z, t) \frac{\partial F(x, z)}{\partial x} \end{aligned} \tag{25}$$

$$c^*(x, z, t)|_{t=0} = -F(x, z) \tag{26}$$

$$\frac{\partial c^*(x, z, t)}{\partial z} \Big|_{z=0} = 0 \tag{27}$$

$$c^*(x, z, t)|_{z=1} = 0 \tag{28}$$

$$c^*(x, z, t)|_{x=0} = 0 \tag{29}$$

$$\frac{\partial c^*(x, z, t)}{\partial x} \Big|_{x=1} = 0 \tag{30}$$

A filtered boundary-homogeneous system is obtained where $G(x, z, t)$ is a new source term incorporating operators of the original equation which were not represented by the filter.

Following the GITT formalism, the potential is expressed as an expansion of normalized eigenfunctions, $\bar{\Psi}_i(z)$ and $\bar{\Phi}_m(x)$, making it possible to build a transform-inverse pair as follows:

$$\bar{c}_{im}^*(t) = \int_0^1 \int_0^1 c^*(x, z, t) \bar{\Psi}_i(z) \bar{\Phi}_m(x) dx dz \tag{31}$$

$$c^*(x, z, t) = \sum_{i=1}^{\infty} \sum_{m=1}^{\infty} \bar{c}_{im}^*(t) \cdot \bar{\Psi}_i(z) \bar{\Phi}_m(x) \tag{32}$$

Next, applying the operator $\int_0^1 \int_0^1 \bar{\Psi}_j(z) \bar{\Phi}_n(x) dx dz$ to the system (24)–(30) and making use of the orthogonal properties of the eigenfunctions, one obtains an infinite system of time-dependent ODEs for the coefficients $\bar{c}_{im}^*(t)$,

$$\frac{d\bar{c}_{im}^*(t)}{dt} + \sum_{j=1}^{\infty} \sum_{n=1}^{\infty} [A \cdot D_{ij} E_{mn} + H_{ij} \delta_{mn} - B \cdot R_{mn} P_{ij}] \cdot \bar{c}_{jn}^*(t) = \bar{g}_{im}(t) \tag{33}$$

$$\bar{c}_{im}^*(0) = -s_{im} \tag{34}$$

where

$$\bar{g}_{im}(t) = g1_{im}(t) + g2_{im}(t) + g3_{im}(t) \tag{35}$$

$$s_{im} = \int_0^1 \int_0^1 \bar{\Psi}_i(z) \bar{\Phi}_m(x) F(x, z) dx dz \tag{36}$$

$$g1_{im}(t) = - \int_0^1 \int_0^1 k_{zz}(z, t) \bar{\Phi}_m(x) \frac{\partial F(x, z)}{\partial z} \frac{d\bar{\Psi}_i(z)}{dz} dx dz \tag{37}$$

$$g_{2im}(t) = \int_0^1 \int_0^1 B.k_{xx}(z, t) \frac{\partial^2 F(x, z)}{\partial x^2} \bar{\Psi}_i(z) \bar{\Phi}_m(x) dx dz \quad (38)$$

$$\frac{d\Psi_i(z)}{dz} \Big|_{z=0} = 0 \quad (47)$$

$$g_{3im}(t) = - \int_0^1 \int_0^1 A.u(z, t) \frac{\partial F(x, z)}{\partial x} \bar{\Psi}_i(z) \bar{\Phi}_m(x) dx dz \quad (39)$$

$$\Psi_i(z) \Big|_{z=1} = 0 \quad (48)$$

$$D_{ij}(t) = \int_0^1 u(z, t) \bar{\Psi}_i(z) \cdot \bar{\Psi}_j(z) dz; \quad (40)$$

$$\frac{d^2 \Phi_m(x)}{dx^2} + \lambda_m^2 \Phi_m(x) = 0 \quad (49)$$

$$H_{ij}(t) = - \int_0^1 k_{zz}(z, t) \frac{d\bar{\Psi}_i(z)}{dz} \frac{d\bar{\Psi}_j(z)}{dz} dz \quad (41)$$

$$\frac{d\Phi_m(x)}{dx} \Big|_{x=1} = 0 \quad (51)$$

yielding respectively the eigenvalues, normalized eigenfunctions and norms,

$$P_{ij}(t) = \int_0^1 k_{xx}(z, t) \bar{\Psi}_j(z) \bar{\Psi}_i(z) dz \quad (42)$$

$$\mu_i = \frac{(2i - 1)}{2} \pi \quad (52)$$

$$R_{mn} = \int_0^1 \bar{\Phi}_n(x) \frac{d^2 \bar{\Phi}_m(x)}{dx^2} dx \quad (43)$$

$$\bar{\Psi}_i(z) = \cos(\mu_i \cdot z) / \sqrt{N_i} \quad (53)$$

$$E_{mn} = \int_0^1 \bar{\Phi}_n(x) \frac{d\bar{\Phi}_m}{dx} dx \quad (44)$$

$$N_i = \int_0^1 \Psi_i^2(z) dz \quad (54)$$

$$\lambda_m = \frac{(2m - 1)}{2} \pi \quad (55)$$

Once the system (33)–(34) is solved, the final potential is then recovered as:

$$c(x, z, t) = \sum_{i=1}^{\infty} \sum_{m=1}^{\infty} \bar{c}_{im}^*(t) \cdot \bar{\Psi}_i(z) \bar{\Phi}_m(x) + F(x, z) \quad (45)$$

$$\bar{\Phi}_m(x) = \sin(\lambda_m \cdot x) / \sqrt{N_m} \quad (56)$$

The above solution is exact but obviously cannot be accomplished without reducing it to a finite system. An approximate solution, however, can be achieved by truncating the series to an order sufficiently large to reach a certain prescribed accuracy.

The eigenfunctions and related eigenvalues for both vertical and longitudinal directions come from Sturm–Liouville auxiliary problems satisfying the related boundary conditions:

$$\frac{d^2 \Psi_i(z)}{dz^2} + \mu_i^2 \Psi_i(z) = 0 \quad (46)$$

$$N_m = \int_0^1 \Phi_m^2(x) dx \quad (57)$$

A generalized Sturm–Liouville problem would generate more suitable eigenfunctions and eigenvalues resulting in a faster convergence rate, thus allowing users to reach the prescribed accuracy at a lower truncation order. However, its solution could become more cumbersome, requiring most likely a numerical solution, thereby increasing the processing time which is usually at a premium.

The steady-state filter is obtained by solving the partial differential equation below:

$$Au_f \frac{\partial F(x, z)}{\partial x} = k_{zf} \frac{\partial^2 F(x, z)}{\partial z^2} + Bk_{xf} \frac{\partial^2 F(x, z)}{\partial x^2} \tag{58}$$

$$\left. \frac{\partial F(x, z)}{\partial z} \right|_{z=0} = 0 \tag{59}$$

$$F(x, z)|_{z=1} = 0 \tag{60}$$

$$F(x, z)|_{x=0} = \frac{1}{u_f} \delta(z - z_e) \tag{61}$$

$$\left. \frac{\partial F(x, z)}{\partial x} \right|_{x=1} = 0 \tag{62}$$

which is obtained from the original formulation and representing the wind speed u_f and the eddy diffusivities, k_{zf} and k_{xf} , as constants. This choice, which is quite convenient in order to reach an analytical solution for the filter, does not affect the final fully converged solution, as the difference between the filter and the original potential emerges in the residues, $\bar{g}_{im}(t)$. Obviously, the closer the filter to the original potential, the faster the convergence can be, but one generally needs to compromise in the simplicity of the filter solution. These parameters (k_{zf} and k_{xf}) should have the same magnitude as those occurring at the emission height where the source is located, in order to accelerate the expansion convergence. Indeed, close to the source the plume is still very narrow, and thus, the meteorological parameters are practically constant in the region engulfed by the pollutants.

The system (58)–(62) is readily solved through the Classical Integral Transform Technique by assuming that the potential can be expanded in a series of orthogonal eigenfunctions $\bar{\Psi}_k$. A transform-inverse pair can be built as follows:

$$\bar{F}_k(x) = \int_0^1 \bar{\Psi}_k(z) \cdot F(x, z) dz \quad F(x, z) = \sum_{k=1}^{\infty} \bar{F}_k(x) \bar{\Psi}_k(z) \tag{63}$$

where the eigenfunctions and eigenvalues are the same assigned for the vertical direction in the original problem. Taking the required derivatives of (63) with respect to x and z , replacing them and (46) in (58–62), applying the operator

$$\int_0^1 \bar{\Psi}_k(z) dz \tag{64}$$

and taking into account the orthogonal properties of the eigenfunctions $\bar{\Psi}_k$, one obtains the system below:

$$Bk_{xf} \frac{d^2 \bar{F}_k(x)}{dx^2} - Au_f \frac{d \bar{F}_k}{dx} - k_{zf} \mu_k^2 \bar{F}_k(x) = 0, k = 1, 2, \dots \tag{65}$$

$$\bar{F}_k(x)|_{x=0} = \frac{1}{u(z_e)} \bar{\Psi}_k(z_e) \tag{66}$$

$$\left. \frac{d \bar{F}_k(x)}{dx} \right|_{x=1} = 0 \tag{67}$$

which is readily solved, yielding

$$\bar{F}_k(x) = \frac{\cos(\mu_k z_e)}{\sqrt{N_k} u_f \cdot [q_k^b e^{q_k^b} - q_k^a e^{q_k^a}]} [q_k^b e^{q_k^b} e^{q_k^b x} - q_k^a e^{q_k^a} e^{q_k^a x}] \tag{68}$$

$$q_k^a = \frac{1}{2} \left[\frac{Au_f}{Bk_{xf}} + \Delta_k \right] \tag{69}$$

$$q_k^b = \frac{1}{2} \left[\frac{Au_f}{Bk_{xf}} - \Delta_k \right] \tag{70}$$

$$\Delta_k = \sqrt{\left(\frac{Au_f}{Bk_{xf}} \right)^2 + 4 \mu_k^2 \frac{k_{zf}}{Bk_{xf}}} \tag{71}$$

The exact final expression for the filter is then written as:

$$F(x, z) = \sum_{k=1}^{\infty} \frac{1}{\sqrt{N_k}} \bar{F}_k(x) \cos(\mu_k z) \tag{72}$$

where N_k is the norm. A truncation of (72) at an adequate order provides a suitable formulation for the filter. It is worthwhile to remind that the series expansion for the filter is utterly independent from that associated to the system of the time-dependent differential equations. Hence, the first one can be truncated at a much higher order without any impact on the processing time required to solve that system. A slight increase only occurs in the computational time required to perform the numerical integrations involving the source term.

Before proceeding it is convenient to rewrite system (19)–(20) using a single sum replacing the double one and to condense their contents in a single matrix as follows,

$$\frac{d \bar{c}_h^*(t)}{dt} + \sum_{l=1}^{\infty} w_{hl} \bar{c}_l^*(t) = \bar{g}_h(t), h = 1, 2, 3, \dots \tag{73}$$

$$\bar{c}_h^*(0) = -s_h \tag{74}$$

In this condensed formulation, the eigenvalues μ_i and λ_m are arranged in pairs denoted by the index h as $[\mu(h), \lambda(h)]$. The convergence depends upon the behavior of the transformed potentials $\bar{c}_h^*(t)$, but they are obviously unknown for they belong to the solution being searched. However, on the grounds that for a homogeneous problem they would decay exponentially with the square of the global eigenvalue, a reasonable assumption, provided appropriate filtering is employed [6], is to consider that even for a nonhomogeneous problem this behavior could serve as a guiding pattern.

Under this assumption, the pairs $[\mu(h), \lambda(h)]$ are ordered under the criterion of an increasing value for an equivalent squared-eigenvalue β_h^2 derived from the diagonal of the matrix \mathbf{w}_{hl} . Such a procedure automatically incorporates the physical domain aspect ratio and the $K_{xx}(H)/K_{zz}(H)$ ratio, both relevant parameters to define the ordering of those pairs.

The system (73)–(74) can now be expressed in matrix form as:

$$C'(t) + W(t)C(t) = G(t) \tag{75}$$

$$C(0) = S \tag{76}$$

Once truncated to a finite order, the above system can be numerically solved by using a suitable algorithm such as the subroutine DIVPAG from the IMSL package which works under a user prescribed accuracy.

The ordinary differential system (75)–(76) refers to the general situation when the meteorological parameters u , k_{zz} and k_{xx} change with time. However, in order to perform a comparison with an analytical solution, checking thus the method and its related algorithm, it is necessary to choose time-invariant parameters with the same profiles used by the analytical solution.

For the particular case of time-invariant parameters, \mathbf{W} and \mathbf{G} become constant matrices, and the system has an analytical solution which can be found by using some suitable technique such as variation of parameters, for instance, yielding:

$$\mathbf{C} = [\mathbf{S} - \mathbf{G}\mathbf{W}^{-1}] \cdot e^{\mathbf{W}t} + \mathbf{G}\mathbf{W}^{-1} \tag{77}$$

Since \mathbf{W} is in principle a full general matrix its appearance in a power of e precludes the prompt utilization of (77). Fortunately, it may be transformed into a diagonal matrix, making it thus possible to obtain decoupled solutions. Indeed, it is well known (e.g., Froberg [8]) that when the eigenvalues of a matrix \mathbf{W} are different and nonnull, there exists a regular matrix \mathbf{V} such that $\mathbf{V}^{-1}\mathbf{W}\mathbf{V} = \mathbf{D}$, where \mathbf{D} is

the diagonal matrix formed by the eigenvalues and \mathbf{V} is the matrix of eigenvectors. Therefore,

$$e^{\mathbf{W}t} = \mathbf{V}e^{\mathbf{D}t}\mathbf{V}^{-1} \tag{78}$$

$$\mathbf{C} = [\mathbf{S} - \mathbf{G}\mathbf{W}^{-1}] \cdot \mathbf{V}e^{\mathbf{D}t}\mathbf{V}^{-1} + \mathbf{G}\mathbf{W}^{-1} \tag{79}$$

The matrices \mathbf{V} and \mathbf{D} can be easily evaluated by using a well-tested algorithm such as routine DEVCCG from the IMSL package, while the required matrix inversions and multiplications can be performed as well by subroutines available in the same package. An algebraic solution of this kind has been applied to three-dimensional steady-state laminar forced convection inside rectangular ducts after integral transforming along two spatial coordinates, leaving the remaining one as the independent variable of the transformed ODE system [3]. Later on, Almeida and Cotta [1] applied the same approach to solve a transient two-dimensional advection–diffusion problem in petroleum reservoirs. Quite recently, Wortmann et al. [13] solved a two-dimensional steady-state advection–diffusion equation by also applying the GITT methodology, followed by a Laplace transform to obtain the analytical solution of the resulting ODE system.

The specific test problem treated in this work was chosen aiming at two main goals: the first one focuses on the comparison of the two approaches, i.e., solving system (75)–(76) by the numerical and by the algebraic procedures, seeking for their covalidation and critical analysis of the required CPU time. The second goal is to compare such results with a known analytical solution for a simplified version of the test problem.

In order to accomplish these tasks, matrices \mathbf{W} and \mathbf{G} should be constant, which means that wind and eddy diffusivity profiles are taken as timely invariant. Furthermore, these profiles should match those used in the simplified analytical formulation. Within this context, the analytical solution developed by Huang [11] was obtained, in the form:

$$C(X, Z) = \frac{Q_0(Z.h)^{\frac{(1-n)}{2}}}{\kappa\alpha X} \exp\left[-\frac{a(Z^\alpha + h^\alpha)}{\kappa\alpha^2 X}\right] I_{-\nu}\left[\frac{2a(Zh)^\frac{\alpha}{2}}{\kappa\alpha^2 X}\right] \tag{80}$$

where

$$\alpha = 2 + \gamma - n \tag{81}$$

$$\nu = \frac{(1 - n)}{\alpha} \tag{82}$$

$$U(Z) = aZ^l \tag{83}$$

$$K_{zz}(Z) = \kappa Z^n \tag{84}$$

where $C(X,Z)$ is the effluent concentration, Q_0 is the source intensity, X is the downwind distance from the source, Z is the height above the ground, h is the emission height, $K_{zz}(Z)$ is the vertical eddy diffusivity, $L_{-\nu}$ is the modified Bessel function of the first kind and order $-\nu$, and $U(Z)$ is the mean wind velocity.

This solution is used as a benchmark after setting $a=1$, $n=1$ and reducing it to dimensionless form as follows:

$$c(x, z) = A_1 \frac{1}{x} \exp \left[-B_1 \frac{(z^\alpha + z_c^\alpha)}{x} \right] I_0 \left[C_1 \frac{z^{\frac{\alpha}{2}}}{x} \right] \tag{85}$$

$$A_1 = \left[\frac{H \cdot U(H)}{\kappa \alpha X_m} \right] \tag{86}$$

$$B_1 = \left[\frac{H^\alpha}{\kappa \alpha^2 X_m} \right] \tag{87}$$

$$C_1 = \left[\frac{2H^\alpha h^{\frac{\alpha}{2}}}{\kappa \alpha^2 X_m} \right] \tag{88}$$

where H is vertical length, X_m is longitudinal length, and z_c is the dimensionless emission height.

3 Results and discussions

In this section, a comparison is performed between the results obtained through the numerical and the analytical procedures and the required CPU times to reach them. Moreover, these results are as well critically compared with the known analytical solution [11] for the sake of validation of the algorithms and related codes.

It has been usual in previous works to set the longitudinal eddy diffusivity as a constant for two main reasons: (1) due to a lack of knowledge regarding the behavior of this parameter along x , y and z for the various types of topographies and atmospheric instabilities; (2) on the grounds that its role on the longitudinal dispersion is usually negligible when compared to the advection component.

In this work, however, aiming at the critical comparison with an analytical solution where the longitudinal eddy diffusivity is not taken into account, it is assumed that K_{xx} changes with the height as a fraction R of $K_{zz}(z)$. Under this assumption, slow convergence arising from very small and

constant K_{xx} values would be avoided, since K_{xx} drops together with K_{zz} . In order to check the robustness of the numerical and analytical procedures, they have been both tested with two values of R for different orders of magnitude: 1.0 and 0.02.

The first set of results is in fact intended to illustrate the reason for this choice of the K_{xx} coefficient behavior while attempting to reproduce the idealized situation of no longitudinal dispersion in Huang’s model [11]. Figure 1 depicts longitudinal concentration profiles for two different assumptions: a constant K_{xx} and a K_{xx} varying as a constant fraction $R=1$ of $K_{zz}(z)$. For a constant K_{xx} , the pollutant would be dispersed more intensively near the ground level than that one submitted to a K_{xx} proportional to $K_{zz}(Z)$, since in the latter case both diffusivities drop to zero at the ground level. This higher longitudinal dispersion flattens the concentration profile as imposed by mass conservation requirements. Based on this outcome, one can conclude that it would not possible to reproduce the analytical solution by Huang [11] unless a variable K_{xx} is assigned as $R \cdot K_{zz}(z)$, where R should be set sufficiently low.

Next, we provide a covalidation between the numerical and analytical schemes of integral transformation here proposed. Figure 2 shows the transient concentration profile for the point (x_{ref}, z_{ref}) and the steady-state longitudinal and vertical concentration profiles for $R=1.0$. One can observe the excellent agreement between the numerical (dotted line) and the analytical (solid line) techniques. As expected, the profiles intercept at $x=0.15$ with the value $c(x_{ref}, z_{ref}, t_\infty)$. Further numerical values of the related parameters are found in the graph legend.

A comparison between the analytical solution by Huang [11] and those obtained in the present work for $K_{xx}(z) = R \cdot K_{zz}(z)$ and $R=0.02$ is shown in Fig. 3. The analytical and numerical integral transform approaches yield the same results, but the numerical procedure requires a longer execution time as will be later on discussed. When K_{xx} is set constant, it is not so straightforward to perfectly match the analytical solution, as Fig. 4 shows, for the reasons already discussed. The value of R has been set to a low value, aiming at a closer similarity with the model that does not incorporate the longitudinal diffusivity component.

The convergence behavior of the longitudinal concentration profile obtained with the GITT approach for a variable K_{xx} and a ratio $R=0.02$ is depicted in Fig. 5, while a detailed picture at the higher truncation orders around the maximum concentration region is shown in Fig. 6. The related numerical values are shown in Table 1. Convergence to the fourth significant digit was achieved for truncation orders as low as $M=40$, for the position illustrated, while three significant digits are achieved at

Fig. 1 Effect of the coefficient K_{xx} choice on the longitudinal concentration profile

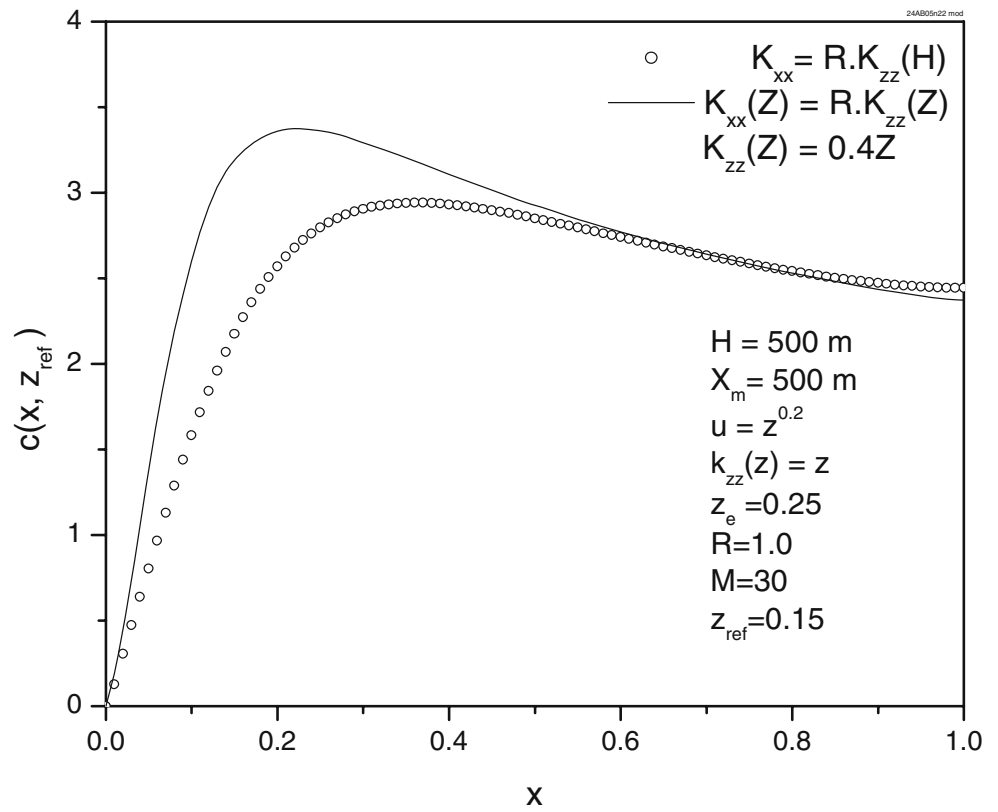


Fig. 2 Transient and steady-state concentration profiles obtained with the numerical and analytical integral transform procedures, with $M=35$

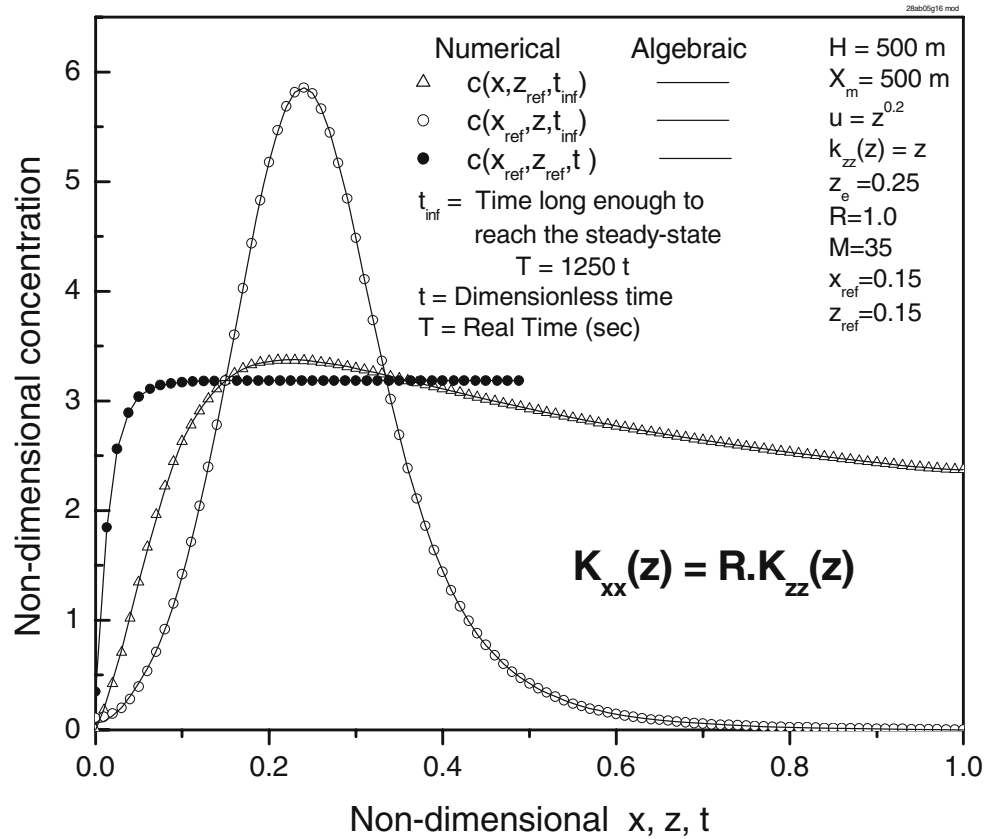
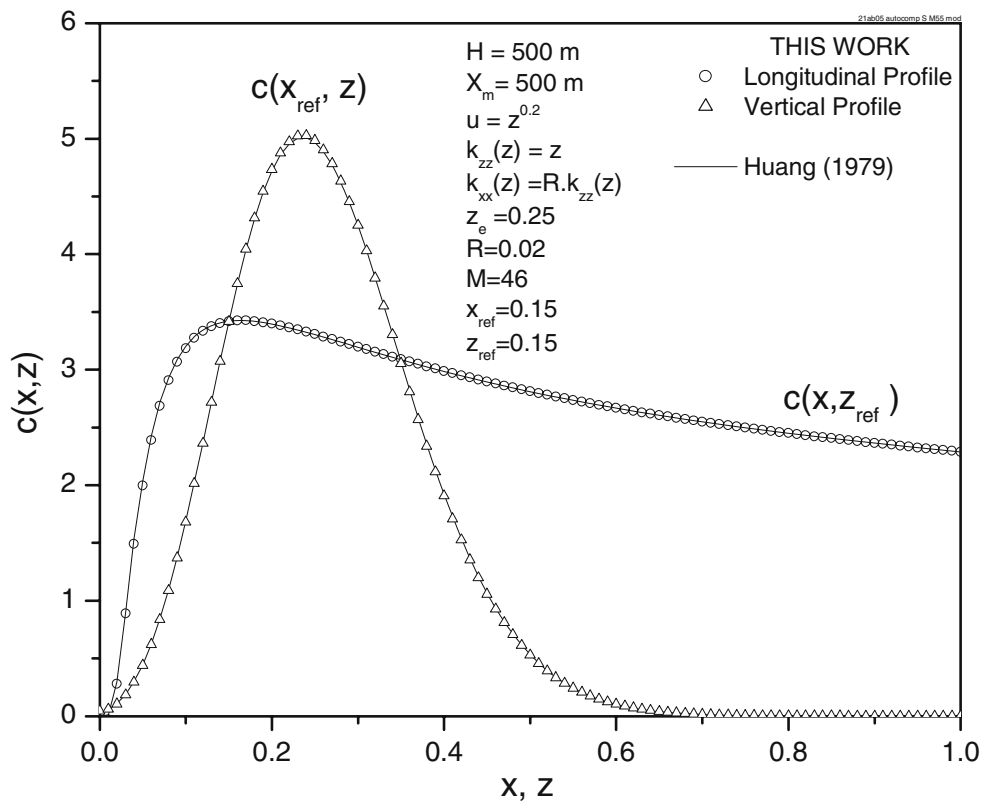


Fig. 3 Steady-state vertical and longitudinal concentration profiles obtained by GITT for $K_{xx}(z)=0.02K_{zz}(z)$, compared with the analytical solution by Huang [11]



much lower orders. In light of the observed negligible deviations between the obtained profiles and the analytical solution in Huang [11], the validation of the algorithm and the related computer program were considered fulfilled.

The required CPU time to run the numerical approach algorithm markedly depends upon the truncation order, the upper limit of the ODE system integration and the degree of stiffness of the system, while for the analytical approach

Fig. 4 Same as Fig. 3 for a constant K_{xx}

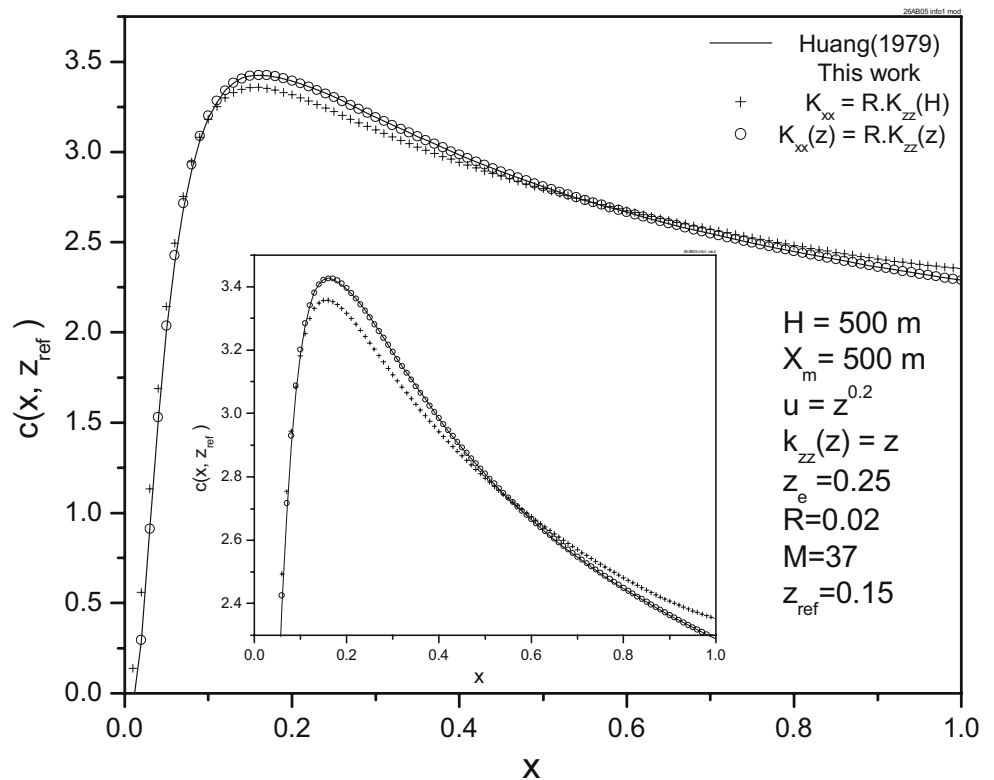
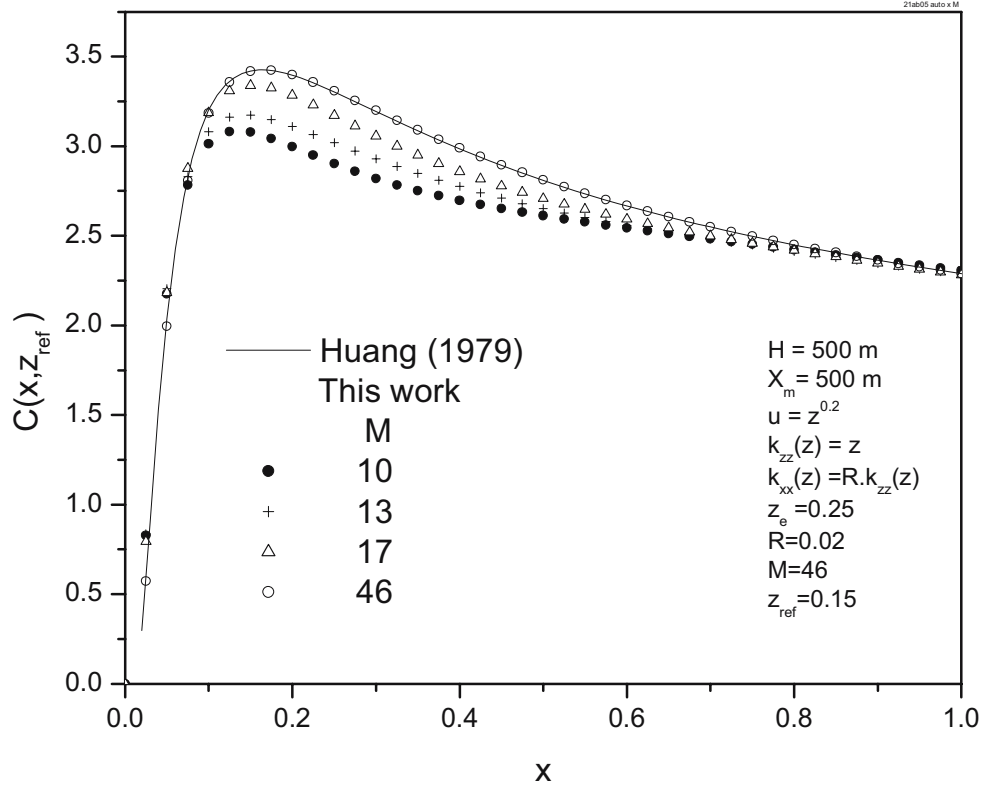


Fig. 5 Comparison of steady-state longitudinal concentration profiles obtained at different truncation orders using the GITT approach, against the analytical solution in Huang [11]



algorithm the only relevant parameter is the final required truncation order.

The impact of the truncation order on the CPU time spent by a 1.8-GHz Pentium processor for both algorithms

written in Fortran is shown in Fig. 7. As an overall impression, the analytical algorithm is about 10 times faster than the numerical procedure. A substantial amount of CPU time might also be consumed for large truncation orders by

Fig. 6 Detail of the convergence evolution at the point (x_{ref}, z_{ref}) of the profile shown in Fig. 5, including a zoom at the high truncation order

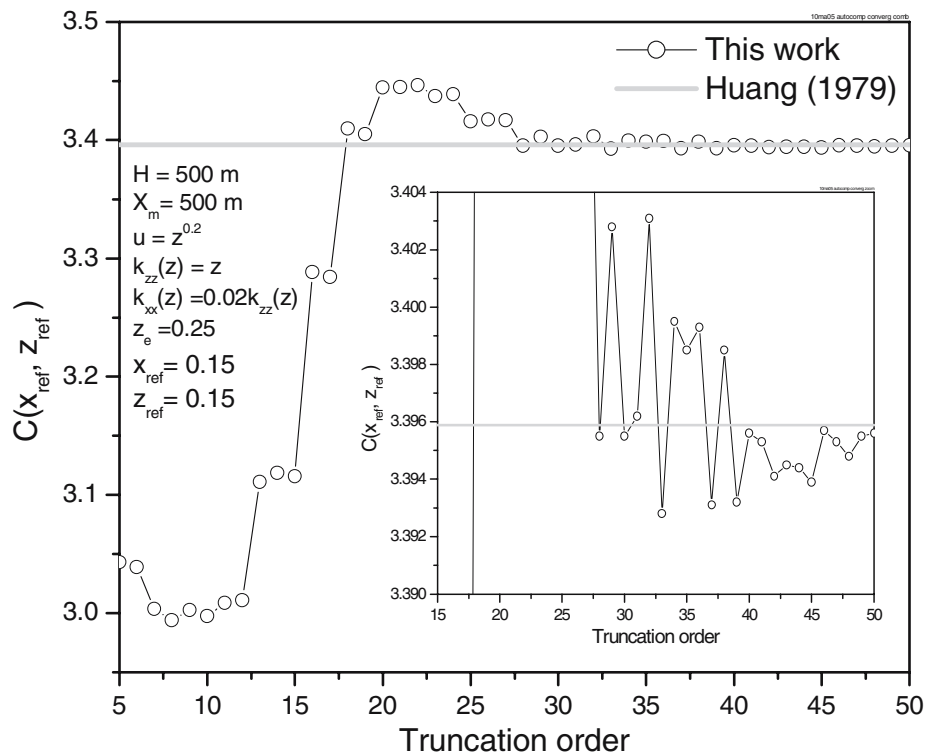


Table 1 Convergence behavior of the concentration at the point [0.2, 0.15] for truncation orders $M=7-50$

M	$C(x_{ref}, z_{ref})$	M	$C(x_{ref}, z_{ref})$	M	$C(x_{ref}, z_{ref})$	M	$C(x_{ref}, z_{ref})$
7	3.0035	18	3.4096	29	3.4028	40	3.3956
8	2.9940	19	3.4050	30	3.3955	41	3.3953
9	3.0026	20	3.4446	31	3.3962	42	3.3941
10	2.9976	21	3.4447	32	3.4031	43	3.3945
11	3.0087	22	3.4464	33	3.3928	44	3.3944
12	3.0108	23	3.4372	34	3.3995	45	3.3939
13	3.1108	24	3.4387	35	3.3985	46	3.3957
14	3.1184	25	3.4158	36	3.3993	47	3.3953
15	3.1157	26	3.4175	37	3.3931	48	3.3948
16	3.2884	27	3.4168	38	3.3985	49	3.3955
17	3.2843	28	3.3955	39	3.3932	50	3.3956

the routines carrying out the determination of the eigenvalues, eigenvectors and matrices inversion in the analytical approach algorithm, and their optimization might be considered in future implementations.

Low R ratios lead the problem towards a less diffusive formulation making the ODE system more stiff, thus increasing the required CPU time, as shown by the given examples for $R=1.0$ and 0.02 , where K_{xx} has been kept proportional to $K_{zz}(z)$ along the whole vertical domain. When K_{xx} is kept constant as a fraction of a $K_{zz}(z)$ occurring at a chosen height z_{ref} , the system becomes less stiff even for the very same values of R , mainly when it is low, as

shown in Fig. 8, for $z_{ref}=H$. This happens since near the ground level the problem becomes highly diffusive, for the wind speed becomes very low, while K_{xx} keeps its constant value.

4 Conclusions

A general two-dimensional transient advection–diffusion equation involving time-dependent parameters such as wind speed and eddy diffusivities generated, after a double integral transformation, a system of ODEs where the related

Fig. 7 CPU time (1.8 GHz Pentium processor) to solve the transformed ODE system using subroutine DIVPAG (IMSL Library) and for the proposed analytical approach as a function of truncation order, M

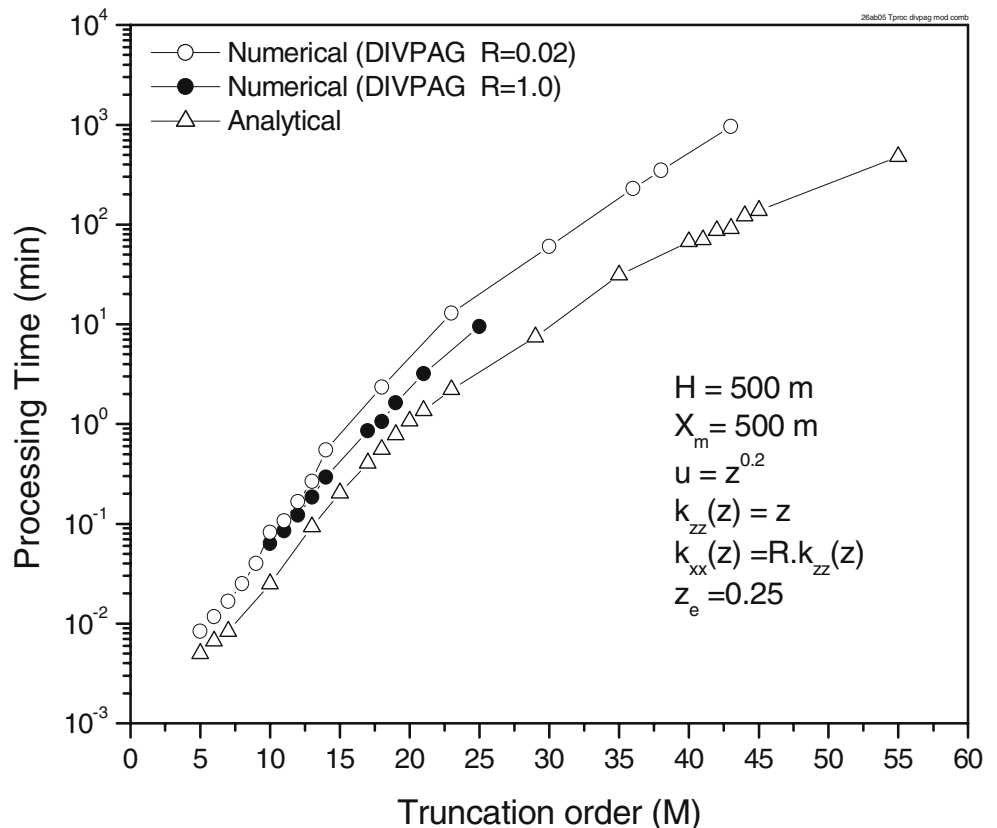
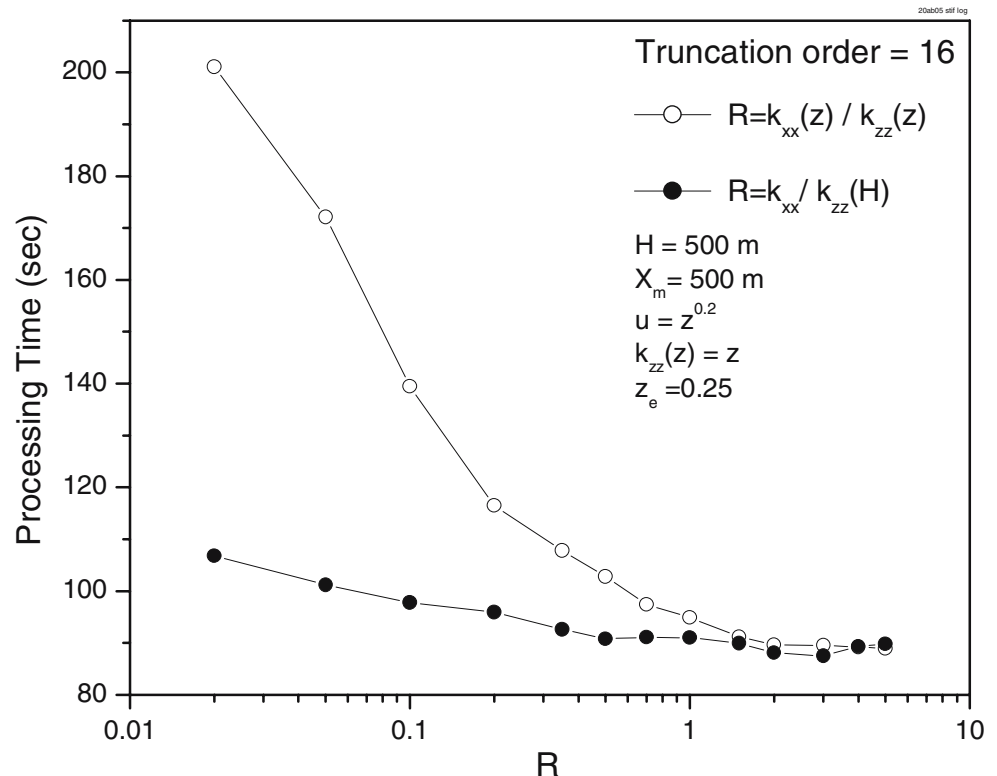


Fig. 8 Influence of the K_{xx}/K_{zz} ratio on the CPU time (1.8 GHz Pentium processor) using subroutine DIVPAG (IMSL Library) for the transformed ODE system solution



coefficients matrices remain as well time-dependent. For this case, a suitable numerical algorithm such as the routine DIVPAG from the IMSL package should be used, as successfully accomplished in the present work. However, depending on the parameters of the original problem, the system may become more stiff, demanding a higher processing time to solve it. Therefore, whenever the matrices of the transformed problem are constant, it becomes much more efficient to apply an analytical approach to solve the ODE system. Indeed, besides the intrinsic robustness of an analytical method, one can directly compute the potentials for any given elapsed time without the need to perform a numerical integration up to that value of the time variable. These advantages make it preferable to use the analytical approach as a benchmarking tool for cross-checking purposes of developed algorithms in more complex formulations. Both approaches have been employed in the present work for a test problem involving constant matrices, yielding identical results, thus confirming the robustness of the algorithms and specifically of the numerical code for the more general case of time-dependent matrices.

Besides, the solution of a problem formulation incorporating a low longitudinal-to-vertical eddy diffusivity ratio was provided by both approaches, and has been compared with a known exact solution for the simplified formulation without the longitudinal diffusion term, with excellent overall agreement. It has been shown that to accomplish this comparison task the longitudinal diffusivity should

have a behavior similar to the vertical one, in vanishing at the ground boundary.

Finally, the influence of the ODE system stiffness on the demanded CPU time to numerically solve it through the routine DIVPAG from the IMSL library has been assessed and analyzed by varying the longitudinal-to-vertical eddy diffusivity ratio.

It should be recalled that the present integral transform numerical scheme could be further optimized in terms of computational performance by implementing the adaptive procedure for automatic truncation order reduction and control along the ODE system integration, as described in Cotta [4] and Cotta and Mikhailov [6], but to allow for a direct comparison with the analytical scheme alternative, the truncation orders were kept constant along the integration procedure in both cases. Also, more elaborate filtering schemes could provide a substantial enhancement in convergence behavior to further improve the computational performance of either of the algorithms here implemented, such as the local instantaneous filtering strategy discussed in Gondim et al. [9].

References

- Almeida, A. R., & Cotta, R. M. (1995). Integral transform methodology for convection–diffusion problems in petroleum reservoir engineering. *International Journal of Heat and Mass Transfer*, 38(18), 3359–3367.

2. Almeida, G. L., Pimentel, L. C. G., & Cotta, R. M. (2003). analysis of pollutants atmospheric dispersion from a point source using integral transforms. *Proceedings of the 3rd International Conference on Computational Heat and Mass Transfer*, May 26–30, 2003, Banff, Canada.
3. Aparecido, J. B., & Cotta, R. M. (1990). Thermally developing laminar flow inside rectangular ducts. *International Journal of Heat and Mass Transfer*, 33(2), 341–347.
4. Cotta, R. M. (1993). *Integral Transforms in Computational Heat and Fluid Flow*. CRC Press, EUA.
5. Cotta, R. M. (1998). *The Integral Transform Method in Thermal and Fluids Science and Engineering*. New York: Ed. Begell House Inc.
6. Cotta, R. M., & Mikhailov, M. D. (1997). *Heat Conduction: Lumped Analysis, Integral Transforms, Symbolic Computation*. New York: John Wiley & Sons.
7. Cotta, R. M., & Özisik, M. N. (1986). Laminar forced convection in ducts with periodic variation of inlet temperature. *International Journal of Heat and Mass Transfer*, 29(10), 1495–1501.
8. Froberg, C. E. (1966). *Introduction to Numerical Analysis*. London: Addison-Wesley.
9. Gondim, R. R., Macedo, E. N., & Cotta, R. M. (2007). Hybrid solution for transient internal convection with axial diffusion: Integral transforms with local instantaneous filtering. *Int. J. Num. Meth. Heat & Fluid Flow*, 17(4).
10. Guerrero, J. S. P., Pimentel, L. C. G., Heilbron Filho, P. F. L., & Cataldi, M. (2001). Study of pollutant transport in surface boundary layer by Generalized Integral Transform Technique. *Proc. of the 2nd Conference on Computational Heat and Mass Transfer. COPPE/UFRJ Brazil October; also, Hybrid Meth. Eng.*, Vol. 3, nos. 2 & 3.
11. Huang, C. H. (1979). A theory of dispersion in turbulent shear flow. *Atmospheric Environment*, 13, 453–463.
12. Moreira, D. M., Vilhena, M. T., Tirabassi, T., Buske, D., & Cotta, R. M. (2005). Near source atmospheric pollutant dispersion using the new GILTT method. *Atmospheric Environment*, 39(34), 6289–6294.
13. Wortman, S., Vilhena, M. T., Moreira, D. M., & Buske, D. (2005). A New analytical approach to simulate the pollutant dispersion in the PBL. *Atmospheric Environment*, 39(12), 2187–2194.